

# Think2Drive: Efficient Reinforcement Learning by Thinking in Latent World Model for Quasi-Realistic Autonomous Driving (in CARLA-v2)

Qifeng Li\* Xiaosong Jia\* Shaobo Wang Junchi Yan†

Department of Computer Science and Engineering, Shanghai Jiao Tong University

{liqifeng, jiaxiaosong, shaobowang1009, yanjunchi}@sjtu.edu.cn

\* Equal contributions †Correspondence author

## Abstract

*Real-world autonomous driving (AD) especially urban driving involves many corner cases. The lately released AD simulator CARLA v2 adds 39 common events in the driving scene, and provide more quasi-realistic testbed compared to CARLA v1. It poses new challenge to the community and so far no literature has reported any success on the new scenarios in V2 as existing works mostly have to rely on specific rules for planning yet they cannot cover the more complex cases in CARLA v2. In this work, we take the initiative of directly training a planner and the hope is to handle the corner cases flexibly and effectively, which we believe is also the future of AD. To our best knowledge, we develop the first model-based RL method named Think2Drive for AD, with a world model to learn the transitions of the environment, and then it acts as a neural simulator to train the planner. This paradigm significantly boosts the training efficiency due to the low dimensional state space and parallel computing of tensors in the world model. As a result, Think2Drive is able to run in an expert-level proficiency in CARLA v2 within 3 days of training on a single A6000 GPU, and to our best knowledge, so far there is no reported success (100% route completion) on CARLA v2. We also propose CornerCase-Repository, a benchmark that supports the evaluation of driving models by scenarios. Additionally, we propose a new and balanced metric to evaluate the performance by route completion, infraction number, and scenario density, so that the driving score could give more information about the actual driving performance.*

## 1. Introduction

Autonomous driving (AD) [18], especially urban driving, requires self-driving vehicles to handle regular tasks e.g. lane following and simple turns, as well as engage with traffic participants [21–23] and adapt to complex and dynamic traffic scenarios. With the increasing requirements from L2

level to L4, driving agents should be able to deal with high traffic complexity and intricate road topology.

There have emerged simulators e.g. HighwayEnv [26] and CARLA v1 [8] for the development and validation of AD models. In these early simulators, the behaviors of environment agents are usually simple and the diversity and complexity of road conditions are usually limited, bearing a gap to real-world driving. Specifically, most of their tasks can be effectively addressed by rule-based approaches via basic skills like lane following, adherence to traffic signs, and collision avoidance, which is however well below the difficulty level of urban driving. For instance, in CARLA v1, the rule-based Autopilot with only hundreds of lines of code could achieve nearly perfect performance [20]. Thus methods developed for, or verified in these environments are possibly not able to deal with many common real-world traffic scenarios, which seriously limit their practical value.

Accordingly, CARLA v2 [2] was released in November 2022, encompassing 39 real-world corner cases in addition to its v1 version of 10 cases. For instance, there are scenarios where the ego vehicle is on a two-way single-lane road and encounters a construction zone ahead. It requires the ego agent to invade the opposite lane when it is sufficiently clear, circumventing the construction area, and promptly merging back into the original lane afterward. In particular, corner cases, as their names suggest, are sparse in both the real world and the routes provided by CARLA v2, posing a long-tail problem for learning.

Being aware of the difficulty of their benchmark, the CARLA team also provides several human demonstrations of completing these scenarios. Though humans could effortlessly navigate such scenarios, it is highly non-trivial to write into rules, not to mention adopting the popular imitation learning methods [19] with few samples as succeed in CARLA v1. Due to its much-increased difficulty, widely used rule-based experts like autopilot [20] and learning-based experts like Roach [38] (by model-free RL) both can not work in CARLA v2 at all. Up to date, there is no success reported on CARLA v2, one year after its release.

In this paper, we aim to obtain the driving policy under such quasi-realistic AD simulations by learning, ambitiously with a model-based RL [15] approach which hopefully would enjoy two merits: data efficiency and flexibility against complex scenarios. It is well known that developing model-based RL can be nontrivial, depending on the specific domain area. It not only involves difficulties intrinsic to AD such as complex road conditions and highly interactive behaviors in long-tailed distributions, but also engineering problems of CARLA e.g. collecting massive samples efficiently from a cumbersome simulator. In contrast, to our best knowledge, existing RL methods for AD [3, 38] are all model-free [27, 31], which would inherently suffer from data inefficiency due to the complexity in CARLA v2.

We model the environment’s transition function in AD using a world model [11, 14, 17] and employ it as a neural network simulator, to make the planner ‘think’ to drive (**Think2Drive**) in the learned latent space. In this way, the data efficiency could be significantly increased since the neural network could in parallel conduct hundreds of rollouts with a much faster iteration speed compared to the physical simulator i.e. CARLA. However, even with the state-of-the-art model-based methods [17], it is still highly non-trivial to adopt them for autonomous driving which has its unique characteristics as mentioned below compared to Atari or MineCraft as done in [17]. Specifically, we consider three major obstacles and our corresponding techniques in model-based RL for quasi-realistic AD.

**1) Policy degradation.** There might exist contradictions among optimal policies of different scenarios. Consequently, the driving model will be easily trapped in the local optima. To mitigate this issue, we randomly re-initialize all weights of the planner in the middle of training while keeping the world model unchanged inspired by [28], allowing the planner to escape local optima for policy degradation preventing. As the world model can provide the planner with accurate and dense rewards after being well-trained, the reinitialized planner can better deal with the cold-start problem.

**2) Long-tail nature.** As mentioned above, the long-tail nature of quasi-realistic AD tasks poses a significant challenge for the planner to handle all the corner cases. To this end, we implement an automated scenario generator that can generate scenarios based on road situations, thus providing the planner with abundant, scenario-dense data. We further design a termination-priority replay strategy, ensuring that the world model and planner prioritize exploration on long-tailed valuable states.

**3) Vehicle heading stabilization.** For a learning-based planner, maintaining the same action over a long time is hard. However, stability and smoothness of control are required in the context of autonomous driving, such as maintaining a steady steer value on a straight lane. Therefore,

we also introduce a steering cost function to stabilize the vehicle’s heading.

Beyond these three major obstacles, the training of a model-based AD planner also encounters challenges such as initial startup difficulties, delayed learning signals, etc. We address them brick by brick, with a **detailed discussion provided in Sec. 3.3**. By developing all the above techniques, we manage to establish our model, **Think2Drive**, which has achieved **the pioneering feat of successfully addressing all 39 quasi-realistic scenarios within 3 days of training on a single GPU A6000**. **Think2Drive** aims to serve as an excellent planning module or teacher model for the development of advanced learning-based models for complex urban driving.

**The highlights of the paper are as follows.** 1) To our best knowledge, we are the first model-based RL approach for AD in literature that manages to handle quasi-realistic scenarios with tailored bricks including **resetting technique, automated scenario generation, termination-priority replay strategy, steering cost function**, etc.; 2) We propose a new and balanced metric to evaluate the performance by route completion and infraction number per kilometer; 3) Experimental results on CARLA V2 and the proposed **CornerCaseRepository** benchmark show the superiority of our approach.

## 2. Related Works

**Model-based Reinforcement Learning.** These methods explicitly utilize a world model to learn the transition of the environment and make the actor purely interact with the world model to improve data efficiency. PlaNet [14] proposes the recurrent state-space model (RSSM) to model both the deterministic and stochastic part of the environment followed by many later works [13, 16, 17, 30]. For instance, Dreamer [13], Dreamer2 [16], and Dreamer3 [17] progressively improve the performance of the world model based on RSSM. Notably, DreamerV3 achieves state-of-the-art performance across multiple tasks including Minecraft, DMLab, and Crafter, without the need of parameter tuning by employing techniques including symlog loss and free bits. Daydreamer [37] further extends the application of model-based approaches to physical robots.

We note that model-based RL is especially fit for AD since (i) the super data efficiency of the model-based method is the key to deal with the long-tailed issue of AD while the physical simulator is usually burdensome; (ii) the transition of AD scenes under rasterized BEV is relatively easy to learn compared to Atari or MineCraft, which means one would be able to train a highly accurate world model. However, it is non-trivial to directly adopt the model-based approach for self-driving because of some unique characteristics such as long-tail nature and reward contradictions.

**Learning-based Agents in CARLA.** In the traditional AD stack, the decision-making process is usually rule-based [33]. Though manual rules enable explainable control over the vehicle, it is difficult to deal with gradually appearing long-tailed corner cases. Learning-based agents aim to overcome the obstacle by computations. However, it is expensive and unsafe to directly test learning-based agents in the real world. The simulator CARLA [8] provides a basic environment. Among these works, [9] demonstrates the effectiveness of an end-to-end imitation learning (IL) baseline using a single-camera input. Additionally, approaches e.g. CIL [6] and CILRS [7] utilize branched action heads, selecting branches based on high-level directional commands. LBC [4] involves mapping camera images to waypoints, emulating a mid-to-mid imitation learning agent, which, in turn, utilized bird’s-eye view (BEV) data to generate future waypoints. [5] explores the utilization of BEV data as input for DDQN [34], TD3 [10], and SAC [12], with the added step of pre-training the image encoder on expert trajectories. [29] investigates the integration of IL with reinforcement learning. Roach [38] is the state-of-the-art model-free RL agent widely used as the expert model of recent end-to-end AD [24, 25, 35, 36], yet it fails to handle the CARLA v2 (Details in Sec. 4.4).

However, even Roach is not able to solve CARLA v2 and thus we propose Think2Drive, a model-based RL method, with tailored designs for quasi-realistic urban driving.

### 3. Methodology

#### 3.1. Problem Formulation with Model-based RL

As our focus is on planning, we use the input of privileged information  $x_t$  including bounding boxes of surrounding agents and obstacles, HD-Map, states of traffic lights, etc, eliminating the influence of perception. The required output is the control signals:  $A$  : throttle, steer, brake.

We construct a planner model  $\pi_\eta$  which outputs action  $a_t$  based on current state  $s_t$  and construct a world model  $F$  to learn the transition of the driving scene so that the planner model could drive and be trained by “think” instead of directly interacting with the physical simulator. The iteration process of “think” is as follows: given an initial input  $x_t$  at time-step  $t$  sampled from the record, the world model encodes it as state  $s_t$ . Then, the planner generates  $a_t$  based on  $s_t$ . Finally, the world model predicts the reward  $r_t$ , termination status  $c_t$ , and the future state  $s_{t+1}$  with  $s_t$  and  $a_t$  as input. The overall pipeline is:

$$s_t \leftarrow F_\theta^{Enc}(x_t), \quad a_t \leftarrow \pi(s_t), \quad s_{t+1} \leftarrow F_\theta^{Pre}(s_t, a_t) \quad (1)$$

By rollouting in the latent state space  $s_t$  of the world model, the planner can think and learn efficiently, reducing the time cost of interacting with the heavy physical simulator.

#### 3.2. World Model Learning and Planner Learning

We use DreamerV3 [17]’s structure and objective to train the world model and planner model.

**World Model Learning.** It has four components [17]:

$$\text{RSSM} \begin{cases} \text{Sequence model:} & h_t = f_\theta(h_{t-1}, z_{t-1}, a_{t-1}) \\ \text{Encoder:} & z_t \sim q_\theta(z_t | h_t, x_t) \\ \text{Dynamics predictor:} & \hat{z}_t \sim p_\theta(\hat{z}_t | h_t) \\ \text{Reward predictor:} & \hat{r}_t \sim p_\theta(\hat{r}_t | h_t, z_t) \\ \text{Termination predictor:} & \hat{c}_t \sim p_\theta(\hat{c}_t | h_t, z_t) \\ \text{Decoder:} & \hat{x}_t \sim p_\theta(\hat{x}_t | h_t, z_t) \end{cases} \quad (2)$$

where **RSSM is to provide an accurate transition function of the environment in latent space and perform efficient rollouts for the planner model.** It decomposes the state representation  $s_t$  into stochastic representation  $z_t$  and deterministic hidden state  $h_t$  based on Eq. (1) to better model the corresponding deterministic and stochastic aspects of the true transition function. The encoder first maps raw input  $x_t$  to latent representation  $z_t$ , then the sequence model predicts the future hidden state  $h_{t+1}$  based on the representation  $z_t$ , action  $a_t$ , and history hidden state  $h_t$ . **The reward predictor forecasts the reward  $r_t$  associated with the model state  $s_t = (h_t, z_t)$  and the termination predictor predicts the termination flags  $c_t \in \{0, 1\}$ , which both provide learning signals for the planner model.** The decoder reconstructs inputs to ensure informative representation and generate interpretable images.

The world model’s training loss [17] consists of:

$$\begin{aligned} \mathcal{L}_{\text{pred}}(\theta) &\doteq -\ln p_\theta(x_t | z_t, h_t) - \ln p_\theta(r_t | z_t, h_t) \\ &\quad - \ln p_\theta(c_t | z_t, h_t) \\ \mathcal{L}_{\text{dyn}}(\theta) &\doteq \max(1, \text{KL}[\text{fz}(q_\theta(z_t | h_t, x_t)) \| p_\theta(z_t | h_t)]) \\ \mathcal{L}_{\text{rep}}(\theta) &\doteq \max(1, \text{KL}[q_\theta(z_t | h_t, x_t) \| \text{fz}(p_\theta(z_t | h_t))]) \end{aligned} \quad (3)$$

where the prediction loss  $\mathcal{L}_{\text{pred}}$  trains both the decoder and the termination predictor via binary cross-entropy. Symlog loss [17] is utilized to train the reward predictor. By minimizing the KL divergence between the prior  $p_\theta(z_t | h_t)$ , the dynamics loss  $\mathcal{L}_{\text{dyn}}$  trains the sequence model to predict the next representation, and the representation loss  $\mathcal{L}_{\text{rep}}$  is used to lower the difficulty of this prediction. The two losses differ in the position of parameter-freeze operation  $\text{fz}(\cdot)$ .

Given a rollout of  $x_{1:T}$ , actions  $a_{1:T}$ , rewards  $r_{1:T}$ , and termination flag  $c_{1:T}$  from records, the overall loss is:

$$\mathcal{L}(\theta) \doteq \mathbb{E}_{q_\theta} \sum_{t=1}^T (\beta_{\text{pred}} \mathcal{L}_{\text{pred}}^t(\theta) + \beta_{\text{dyn}} \mathcal{L}_{\text{dyn}}^t(\theta) + \beta_{\text{rep}} \mathcal{L}_{\text{rep}}^t(\theta)) \quad (4)$$

**Planner Learning.** The planner is learned via an actor-critic [32] architecture, where the planner model serves

as the actor and a critic model is constructed to assist its learning. Benefiting from the world model, the planner model can purely think to drive in the latent space with high efficiency. Specifically, given an input  $x_t$  at  $t$  from the record as a start point, the world model first maps it to  $s_t = (z_t, h_t)$ . Then, the world model and the planner model conduct  $T$  steps exploration:  $\langle \hat{s}_{1:T}, a_{0:T}, r_{0:T}, c_{0:T} \rangle$ . The planner model  $\pi_\eta(a|s)$  tries to maximize the expected discounted return generated by the reward predictor:  $\sum_t \gamma \hat{r}_t$  while the critic learns to evaluate each state conditioned on the planner’s policy:  $V(s_T) \approx \mathbb{E}_{s \sim F_\theta, a \sim \pi_\eta}(R_t)$ .

As the horizon  $T$  gets longer, the accumulated error exponentially grows. Thus, the expected return is clipped by  $T = 15$  and the left return is estimated by the critic:  $R_T = v(s_T)$ . We follow DreamerV3 by employing the trick of bucket-sorting rewards and the two-hot encoding to stably train the critic. Given two-hot encoded target  $y_t = \text{fz}(\text{twohot}(\text{symlog}(R_t^\lambda)))$ , the cross-entropy loss is used to train the critic [17]:

$$\mathcal{L}_{\text{critic}}(\psi) \doteq - \sum_{t=1}^T y_t^\top \ln p_\psi(\cdot | s_t) \quad (5)$$

where the softmax distribution  $p_\psi(\cdot | s_t)$  over equal split buckets is the output of the critic. The reward expectation term for actor training is normalized by moving statistics:

$$\mathcal{L}(\theta) \doteq \sum_{t=1}^T \left( \mathbb{E}_{\pi_\eta, p_\theta} \left[ \frac{\text{fz}(R_t^\lambda)}{\max(1, S)} \right] - \beta_{en} H[\pi_\eta(a_t | s_t)] \right) \quad (6)$$

where  $S$  is the decaying mean of the range from their  $5^{th}$  to the  $95^{th}$  batch percentile. More details can be found in [17].

### 3.3. Challenges and Our Devised Bricks

After having the training paradigm determined, it is still not ready to solve the problem, as the autonomous driving scene has very different characteristics compared to Atari or MineCraft, e.g. policy degradation(*Challenge 1*), long-tail nature(*Challenge 2, 3*), and car heading stabilization(*Challenge 4*). These obstacles make it highly non-trivial to adopt MBRL for autonomous driving. To this end, we devise essential Bricks to address them one by one.

**Challenge 1:** As the training progresses, the agent may be trapped in the local optimal policy of easy scenarios. This issue arises from potential contradictions in optimal strategies required for different scenarios. For example, in scenario I where the front vehicle suddenly brakes and scenario II where the planner has to merge into high-speed traffic, the former requires the planner to keep a safe distance from the preceding vehicle, while the latter demands proactive engagement with the front vehicles. Since the former is much easier than the latter, the model can be easily trapped into the local optima of keeping safe distance.

**Brick 1:** We leverage the reset technique [28] in the middle of the training process where we randomly re-initialize all the parameters of the planner, allowing it to escape from the local optima. Notably, different from those model-free methods, the cold-start problem of the reset trick is less damaging since we have the well-trained world model to provide dense rewards.

**Challenge 2:** The 39 scenarios are sparse in the released routes of CARLA v2. It brings a long-tail problem, which incurs skewed exploration over trivial states. Additionally, the released scenarios are coupled with specified waypoints. As a result, the scenarios happen in a few fixed locations, which limits data diversity.

**Brick 2:** We implement an automated scenario generator. Given a route, it can automatically split the route into multiple short routes and generate scenarios according to the road situation. As a result, the training process is able to acquire numerous shorter routes with dense scenarios. Besides, we build a benchmark **CornerCaseRepository** for evaluation which could estimate the detailed capabilities under each scenario while the official test routes are too long and thus their results are difficult to analyze.

**Challenge 3:** Valuable transitions occur non-uniformly over time and thus it is inefficient to train the world model under uniform sampling. For example, in a 10-second red traffic light, an optimal policy with a decision frequency of 10 FPS will produce 100 consecutive frames of low-value transition, indicating that the exploration space of the planner remains highly imbalanced and long-tailed.

**Brick 3:** One kind of valuable transition can be easily located, i.e. the  $K$  frames preceding the termination frame of an episode. Such terminations are either due to biases in the world model or exploration behavior, both of which could be especially valuable for the world model to learn the transition functions. Consequently, we employ a termination-priority sampling strategy where we either randomly sample or sample at the termination state with equal probability.

**Challenge 4:** For reinforcement learning agents, particularly stochastic agents, maintaining a consistent action over an extended trajectory presents a challenge. For example, as could be observed in the demo of Roach [38], the head of the ego vehicle would fluctuates even when driving in the straight road. However, this consistency is often a requisite in the context of autonomous driving.

**Brick 4:** To address this, we incorporate a steering cost function into the training of our agent. This cost function has enabled our model to achieve stable navigation.

**Challenge 5:** The difficulty varies across scenarios. Directly training an agent with all scenarios may result in an excessively steep learning curve. Specifically, for these safety-critical scenarios requiring subtle control of the ego vehicles, it has a high risk of having violations or collisions and thus the model would be trapped in the over-



conservation local optima (as evidenced in Sec. 4.7).

**Brick 5:** Inspired by curriculum learning [1], prior to undertaking unified training across all scenarios, we conduct a warm-up training stage for the RL model, using simple lane following and simple-turn scenarios so that the model has the basic driving skills and then we let it deal with these complex scenarios.

*Challenge 6:* The dynamics of the driving environment are relatively stable compared to many stochastic tasks. The world model can gradually learn a more accurate transition function of the environment and generate more precise rewards for the planner. While the agent network relies on delayed, world model-generated rewards, requiring a longer time to converge. If the training ratio for both the world model and the agent is set equivalently, as is common in many tasks, this could decelerate the training process.

**Brick 6:** We set an incremental train ratio for the planner model where at the end the train ratio of the planner will be four times that of the world model, to expedite the convergence speed.

*Challenge 7:* RL training necessitates efficient exploration and environment resets, while the time cost of every reset in CARLA is unacceptable ( $> 40s$  to load the route and instantiate all scenarios).

**Brick 7:** We wrap CARLA as an RL environment with standardized APIs and boost its running efficiency via asynchronous reloading and parallel execution. Details can be found in Fig. 4, Sec. 4.7

## 4. Experiment

### 4.1. CARLA Leaderboard v2

CARLA Leaderboard v2 is based on the CARLA simulator with version bigger than 0.9.13 (V1 on 0.9.10). We evaluate our planner with CARLA 0.9.14. Along with their simulator, CARLA team initially proposed Leaderboard v1, which is composed of basic tasks such as lane following, turning, collision avoidance, and etc. Then, to facilitate quasi-realistic urban driving, they propose CARLA v2, which encompasses a multitude of complex scenarios previously absent in v1. These scenarios pose serious challenges to the ability of autonomous driving methods.

However, since the release of CARLA v2, no team has managed to get a spot to tackle these scenarios, despite the availability of perfect logs scoring 100% on each scenario, provided by the CARLA official platform to aid in related research. In short, four primary reasons are contributing to the difficulty of v2: (1). Extended Route Lengths: In CARLA v2, the routes extend between 7 to 10 kilometers, a substantial increase from the roughly 1-kilometer routes in v1. (2). Complex and Abundant Scenarios: Each route contains around 60 scenarios, which require the driving methods to be able to handle complex road conditions and con-

duct subtle control. (3). Exponential decay scoring rules: The leaderboard employs a scoring mechanism that penalizes infractions through multiplication penalty factors  $< 1$ . In scenarios with extended routes and a multitude of scenarios, models struggle to attain high scores. (4). Limited data: the CARLA team only provides a set of 90 training routes coupled with scenarios while routes randomly generated by researchers, does not have official API support for the placement of scenarios.

### 4.2. CornerCaseRepository Benchmark

As mentioned below, in the official benchmark, multiple scenarios are along a single long route, which makes it hard to train and evaluate the model. To address this deficiency, we introduce the **CornerCaseRepository** benchmark. It consists of 1600 routes for training and 390 routes for evaluation. Every route in **CornerCaseRepository** benchmark contains only one single scenario with a length  $< 300$  meters so that the training and evaluation of different scenarios are decoupled. In the training routes, there are 40 routes for each scenario and 40 routes without any scenarios. The routes are sampled randomly during the RL training process. There are 10 routes for each scenario in evaluation routes. In evaluation mode, the routes are sampled sequentially until all routes have been evaluated. The **CornerCaseRepository** benchmark supports the use of the CARLA metrics (e.g. driving scores, route completion) to analyze the performance of each scenario separately, which provides convenience for debugging.

### 4.3. Weighted Driving Score

As described in Sec. 4.1, the scoring rules of CARLA leaderboard is too rough for driving policy evaluation. For instance, consider a driving model with an average infraction rate of 0.2 per kilometer and a penalty factor of 0.8. Under the hypothetical ideal condition where route completion is 100% for both 5-kilometer and 10-kilometer test routes, the driving scores would be 0.8 and 0.64, i.e., **the longer the distance traveled, the lower the final driving score**. To avoid such counter-intuitive phenomenon, we propose a new metric named **Weighted Driving Score (WDS)**, formed as:

$$\text{WDS} = \text{RC} * \prod_i^m \text{penalty}_i^{n_i} \quad (7)$$

where RC means route completion rate,  $m$  is the total number of types of infractions considered,  $\text{penalty}_i$  refers to the penalty factor for infraction type  $i$  officially defined by CARLA team, and  $n_i = \frac{\text{Number of Infractions}}{\text{Number of Scenarios}}$  (when there is no scenario, we simply set  $n_i = \text{Number of Infractions}$  and in this case Weighted Driving Score=Driving Score.). Weighted Driving Score effectively balances the weight be-

Table 1. **Driving performance and infraction of agents on the proposed SW benchmark.** Mean and standard deviation are over 3 runs.

| Input                  | Method                    | Driving score | Weighted DS     | Route completion | Infraction penalty | Collision pedestrians | Collision vehicles | Collision layout | Red light infraction | Stop sign infraction | Agent blocked    |
|------------------------|---------------------------|---------------|-----------------|------------------|--------------------|-----------------------|--------------------|------------------|----------------------|----------------------|------------------|
| Privileged Information | Roach [38]                | 57.5±9        | 54.8±0.5        | 96.4±1.1         | 0.59±0.28          | 0.85±0.56             | 8.42±4.65          | 0.85±0.51        | 0.56±0.45            | 0.49±0.44            | 0.78±0.31        |
|                        | <b>Think2Drive (Ours)</b> | <b>83.8±1</b> | <b>89.0±0.2</b> | <b>99.6±0.1</b>  | <b>0.84 ± 0.01</b> | <b>0.16±0.01</b>      | <b>1.2±0.5</b>     | <b>0.29±0.02</b> | <b>0.14±0.01</b>     | <b>0.03±0.01</b>     | <b>0.08±0.01</b> |
| Raw Sensors            | Think2Drive+TCP [35]      | 36.40±12.23   | 29.6±0.2        | 85.88±8.26       | 0.41±0.32          | 0.46±0.32             | 9.92±5.12          | 6.75±3.08        | 3.27±1.64            | 5.03±3.82            | 6.18±4.62        |

Table 2. **Performance of Think2Drive on the 39 scenarios in CARLA v2.** The success rate denotes the statistical frequency of achieving 100% route completion with zero instances of infraction. A high success rate does not necessarily mean a high driving score, e.g. in YieldToEmergencyVehicle, the vehicle may finish its route but fails to yield to the emergency vehicle.

| Scenario                             | Success Rate | Scenario                 | Success Rate | Scenario                       | Success Rate | Scenario                                | Success Rate |
|--------------------------------------|--------------|--------------------------|--------------|--------------------------------|--------------|-----------------------------------------|--------------|
| ParkingExit                          | 0.89         | Hazard AtSidelane        | 0.75         | Vinilla Turn                   | 0.99         | Invading Turn                           | 0.90         |
| Signalized LeftTurn                  | 0.95         | Signalized RightTurn     | 0.76         | OppositeVehicle TakingPriority | 0.89         | OppositeVehicle RunningRedLight         | 0.85         |
| Accident                             | 0.81         | Accident TwoWays         | 0.61         | Crossing BicycleFlow           | 0.83         | Highway CutIn                           | 1.0          |
| Construction                         | 0.84         | Construction TwoWays     | 0.72         | Interurban ActorFlow           | 0.83         | InterurbanAdvanced ActorFlow            | 0.8          |
| Blocked Intersection                 | 0.80         | Enter ActorFlow          | 0.65         | NonSignalized RightTurn        | 0.75         | NonSignalizedJunction LeftTurnEnterFlow | 0.67         |
| MergerInto SlowTraffic               | 0.67         | MergerInto SlowTrafficV2 | 0.87         | Highway Exit                   | 0.83         | NonSignalized JunctionLeftTurn          | 0.79         |
| SignalizedJunction LeftTurnEnterFlow | 0.86         | Vehicle TurningRoute     | 0.78         | VehicleTurning RoutePedestrian | 0.75         | Pedestrian Crossing                     | 0.91         |
| YieldTo EmergencyVehicle             | 0.92         | Hard Brake               | 1.0          | Parking CrossingPedestrian     | 0.98         | Dynamic ObjectCrossing                  | 0.94         |
| Vehicles DooropenTwoWays             | 0.78         | HazardAt SideLaneTwoWays | 0.92         | Parked Obstacle                | 0.90         | ParkedObstacle TwoWays                  | 0.91         |
| Static CutIn                         | 0.85         | Parking CutIn            | 0.90         | ControlLoss                    | 0.78         |                                         |              |

tween route completion, the number of infractions, and scenario density, which provides a perspective about the average infractions when agent encountering scenarios.

#### 4.4. Performance

Tab. 1 and Fig. 1 gives results on the **CornerCaseRepository** benchmark. The overall training time on one A6000 GPU with AMD Epyc 7542 CPU - 128 logical cores is 3 days. For the baseline expert model, we implement Roach [38], where we replace our model-based RL model with model-free PPO [31] and keep all the others the same. Both experts are trained on 1600 routes and evaluated on other 390 routes of **CornerCaseRepository** benchmark for 3 runs. Think2Drive outperforms Roach by a large margin, showing the advantages of model-based RL.

We also choose and train an end-to-end baseline namely TCP [35], a lightweight student model with a strong performance on CARLA Leaderboard v1, as the imitation learning agent. We train TCP with 200K frames collected by the Think2Drive expert under different weather. We could

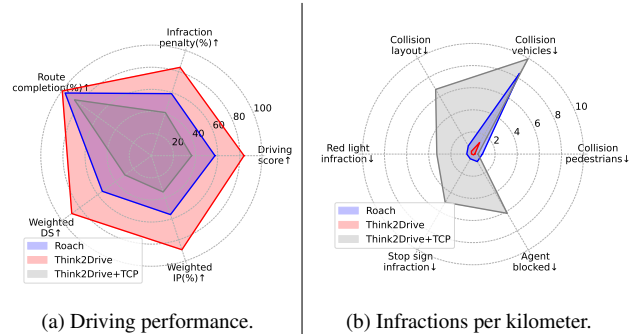


Figure 1. **Driving performance and infractions on CornerCaseRepository benchmark.**

observe that TCP, as a student model with only raw sensor inputs, has a large performance gap with both expert models, as caused by the difficulty of perception parts as well as the imitation learning process.

We also evaluate Think2Drive on the official test routes of CARLA v1 & v2 and compare it with the expert model of Roach. As illustrated in Tab. 3, Think2Drive not only out-

Table 3. **Performance on official test routes.**

| Method             | benchmark | Driving Scores | Weighted Driving Score | Route Complete % |
|--------------------|-----------|----------------|------------------------|------------------|
| Roach (Expert)     | CARLA v1  | 85.0           | —                      | 72.0             |
| Think2Drive (Ours) |           | <b>90.2</b>    | <b>90.2</b>            | <b>99.7</b>      |
| PPO (Expert)       | CARLA v2  | 0.7            | 0.6                    | 1.0              |
| Think2Drive (Ours) |           | <b>56.8</b>    | <b>91.7</b>            | <b>98.6</b>      |

performs Roach in the easier CARLA v1(no scenarios) but also achieves significantly superior performance in the more complex v2 routes. PPO achieved remarkably low scores, a consequence of its rapid convergence to local optima, beyond which the policy ceases to improve further even with the help of the reset technique. We argue that the reason for this phenomenon is that after each reset, PPO has to relearn the policy from the trajectories stored in the replay buffer, which contain inherent reward noise due to the AD characteristics. Conversely, a model-based planner can get accurate and smooth rewards from the world model.

#### 4.5. Infraction Analysis on Hard Scenarios

We analyze the performance of Think2Drive in all scenarios, and give the success rate of the scenarios in Tab. 2.

The scenarios *Accident*, *Construction*, and *HazardAtSidelane* along with their respective *TwoWays* versions, belong to the category of *RouteObstacles* scenarios. In these scenarios, the ego vehicle is required to perform lane changes to maneuver around obstacles, particularly in the case of the *TwoWays* versions where the ego vehicle needs to switch to the opposite lane. Such scenarios demand the ego vehicle to acquire a sophisticated lane negotiation policy, especially in the *TwoWays* scenarios where the ego vehicle must execute lane changing, maneuver around obstacles, and return to its original lane within a short time window. Failed cases in these scenarios typically result from collisions with an opposite car during the process of returning to the original lane after bypassing the obstacles. CARLA v2 generates randomly the opposite traffic flow with speed and interval range within [8, 18] and [15, 50] (typical value, may vary with specific road conditions) in the *TwoWays* scenarios, which may lead to a significantly constrained time window (e.g. less 1 second) for bypassing obstacles when the speed is large while the interval is small. Consequently, the ego vehicle is required to rapidly accelerate from  $speed = 0$  to its maximum speed, and the ego vehicle usually runs at a high speed and is close to the opposite car when returning to its original lane, which leads to a high risk of collisions.

The scenarios *SignalizedLeftTurn*, *CrossingBicycleFlow*, *SignalizedRightTurn* and *BlockedInterSection* belong to *JunctionNegotiate* type. In these scenarios, the ego vehicle has to interrupt the opposite dense car or bicycle flow, merge into the dense traffic flow, and stop at the junction to await road clearance. In CARLA v2, the traffic flow of

Table 4. **The discretized actions.** The continuous action space is decomposed into 30 discrete actions, each for specific values of throttle, steer, and brake. Each action is rational and legitimate.

| Throt. | Brake | Steer | Throt. | Brake | Steer | Throt. | Brake | Steer |
|--------|-------|-------|--------|-------|-------|--------|-------|-------|
| 0      | 1     | 0     | 0.3    | 0     | -0.7  | 0.3    | 0     | 0.7   |
| 0.7    | 0     | -0.5  | 0.3    | 0     | -0.5  | 0      | 0     | -1    |
| 0.7    | 0     | -0.3  | 0.3    | 0     | -0.3  | 0      | 0     | -0.6  |
| 0.7    | 0     | -0.2  | 0.3    | 0     | -0.2  | 0      | 0     | -0.3  |
| 0.7    | 0     | -0.1  | 0.3    | 0     | -0.1  | 0      | 0     | -0.1  |
| 0.7    | 0     | 0     | 0.3    | 0     | 0     | 0      | 0     | 0     |
| 0.7    | 0     | 0.1   | 0.3    | 0     | 0.1   | 0      | 0     | 0.1   |
| 0.7    | 0     | 0.2   | 0.3    | 0     | 0.2   | 0      | 0     | 0.3   |
| 0.7    | 0     | 0.3   | 0.3    | 0     | 0.3   | 0      | 0     | 0.6   |
| 0.7    | 0     | 0.5   | 0.3    | 0     | 0.5   | 0      | 0     | 1     |

these scenarios is configured to be very aggressive, meaning it does not proactively yield to the ego vehicle. The ego vehicle needs to maintain a reasonable distance from other vehicles to avoid collisions. For instance, in the *SignalizedRightTurn* scenario, the ego vehicle is expected to merge into traffic with an interval within [15, 25] meters and a speed within [12, 20] m/s. With a vehicle length of approximately 3 meters, the ego vehicle must not only accelerate rapidly to match the traffic speed in a short time but also simultaneously maintain a safe following distance from preceding and succeeding vehicles.

In scenario *EnterActorFlow*, when the ego vehicle enters the junction, a flow of cars from another junction entry runs a red light, which either will go for the same junction exit to the ego or intersect with the ego’s target route. The speed of this car flow is configured at a high level, ranging between 15 and 20 meters per second. At such high speeds, even minor steering inputs can result in significant changes in the vehicle’s heading, making it challenging for the ego vehicle to maintain frontal stability which significantly increases the risk of collisions.

#### 4.6. Visualization of World Model Prediction

The world model is capable of imaging observation transitions and future rewards based on the agent’s actions, and it can decode them back into the interpretable masks under BEV. Fig. 2 visualizes the initial input and the predicted BEV masks within timestep 50. We could observe that the world model could generate authentic future states, demonstrating one advantage of adopting model-based RL for AD - the transition function is usually easy to learn.

#### 4.7. Ablation Study

We conduct ablation on bricks 1, 3-6(bricks 2 and 7 are foundational for Think2Drive). Fig. 3 presents the results over 500K steps, showing that the absence of any single brick significantly diminishes the performance of Think2Drive. Specifically, bricks 1 and 5 exert the most

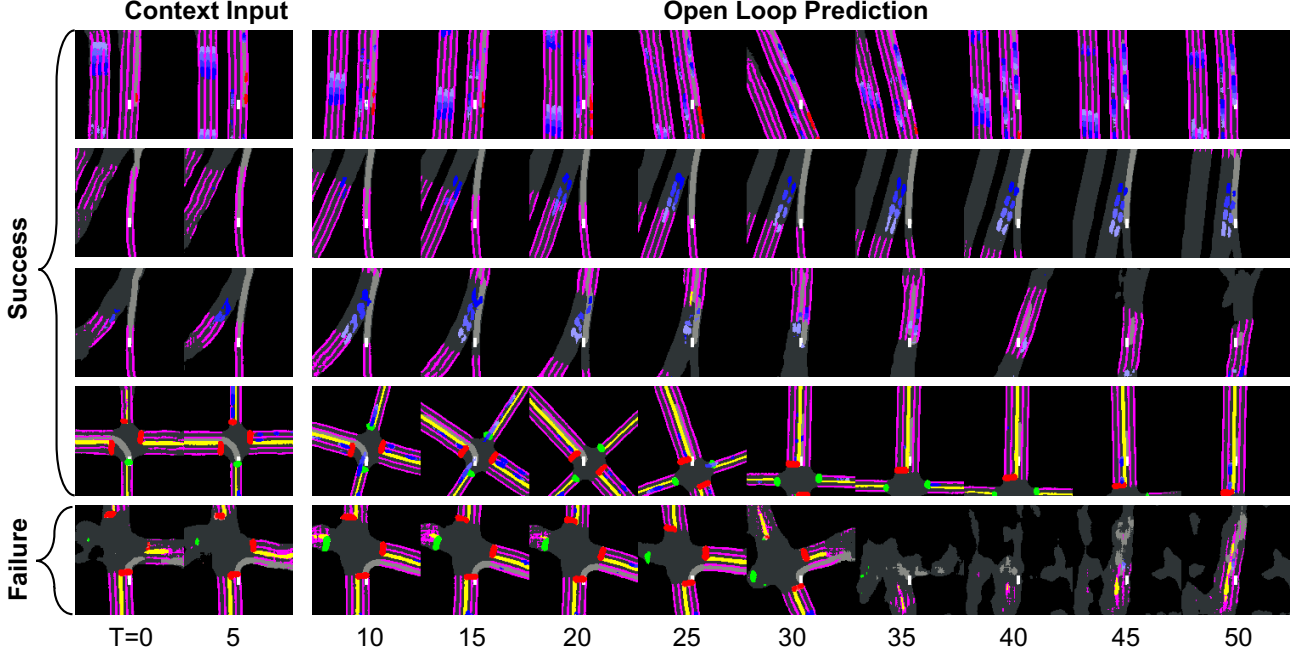


Figure 2. **Example of prediction by the world model based on the first 5 frames.** The model can predict reasonable future frames. In the failure case, the planner runs a red light and the world model terminates the episode, so the following predictions are randomly generated.

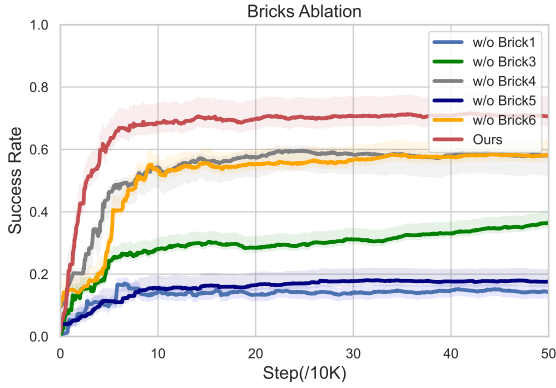


Figure 3. **Ablation of different bricks devised in the paper.**

substantial impact on the final performance. The omission of the warmup stage (brick 5) results in an overly steep learning curve, while forgoing the reset technique (brick 1) predisposes the planner to be stuck in policies only effective in some easy scenarios, both of which lead to the model being trapped in the local optima. The absence of priority sampling (brick 3) is observed to reduce the model’s exploration efficiency, evidenced by the ascending yet slow curve (w/o brick 3). Brick 6 affects the learning efficiency of the planner, where employing a higher training ratio for the planner enables the model to achieve superior performance within the same number of steps. The absence of a steering cost function (brick 4) compromises vehicle steering stability, increasing the propensity for collisions.

## 5. Conclusion

We have proposed a purely learning-based planner, Think2Drive, for quasi-realistic traffic scenarios. Benefiting from the model-based RL paradigm, It can drive proficiently in CARLA v2 with all 39 scenarios within 3 days of training on a single GPU. We also devise tailored bricks such as resetting technique, automated scenario generation, termination-priority replay strategy, and steering cost function to address the obstacles associated with applying model-based RL to autonomous driving tasks. Think2Drive highlights and validates a feasible approach, model-based RL, for quasi-realistic autonomous driving. Our model can also serve as a data collection model, providing expert driving data for end-to-end autonomous driving models.

## 6. Implementation Details

### 6.1. Input&Output Representation.

For the input representation, we utilize BEV semantic segmentation masks  $i_{RL} \in \{0, 1\}^{H \times W \times C}$  as image input, where each channel denotes the occurrence of certain types of objects. It is generated from the privileged information obtained from the simulator and consists of  $C$  masks of size  $H \times W$ . In these  $C$  masks, the route, lanes, and lane markings are all static and thus could be represented by a single mask while those dynamic objects (e.g. vehicles and pedestrians) have  $T$  masks where each mask represents their state at one history time-step. Additionally, we feed speed, con-



Table 5. **Composition of the BEV representation.** Each static object occupies 1 dimension out of the  $C = 34$ , while each dynamic object occupies 4 dimensions out of the  $C = 34$ .

| $C = 34$            |       |     |      |             |            |                      |        |               |          |                     |                          |           |
|---------------------|-------|-----|------|-------------|------------|----------------------|--------|---------------|----------|---------------------|--------------------------|-----------|
| Static( $C_s = 1$ ) |       |     |      |             |            | Dynamic( $C_d = 4$ ) |        |               |          |                     |                          |           |
| road                | route | ego | lane | yellow line | white line | vehicle              | walker | emergency car | obstacle | green traffic light | yellow&red traffic light | stop sign |

Table 6. **Dimension of input/output representation.** The  $T$  temporal masks are from historical time-steps:  $[-16, -11, -6, -1]$ .

| H   | W   | C  | T | M  |
|-----|-----|----|---|----|
| 128 | 128 | 34 | 4 | 30 |

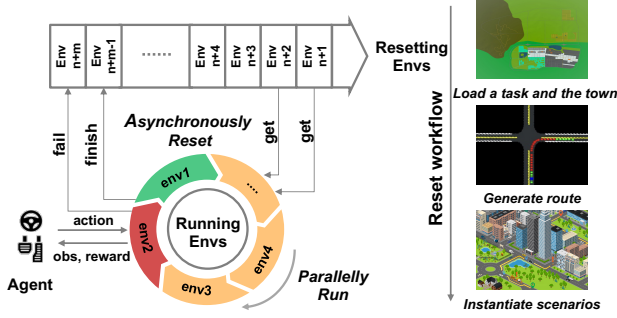


Figure 4. **Procedure of the Wrapped RL Environment.** The right shows the workflow of each reset. In large maps like town12 and town13, the entire reset workflow takes about 1 minute.

trol action, and relative height of the ego vehicle at the previous time steps as input  $v_{RL} \in \mathbb{R}^K$ .

For output representation, we discretize the continuous action spaces of  $throttle \in [0, 1]$ ,  $brake \in [0, 1]$ , and  $steer \in [0, 1]$  into  $M$  actions to reduce the complexity. The actor outputs a one-hot action vector  $a \in \{0, 1\}^M$ . The discretized actions are presented in Tab. 4

The aforementioned hyper-parameters are set as in Tab. 6 while the details about the input information are in Tab. 5.

## 6.2. Simulator Execution Mode

We boost its running efficiency via asynchronous reloading and parallel execution which could avoid the waiting time caused by the long preparation time of starting a new route, as shown in Fig. 4. For each 100K steps of execution, it can reduce about 1 day time cost.

## 6.3. Terminal Condition.

To save the training time cost, we set several termination conditions to terminate episodes in advance. An episode terminates if and only if one of these conditions is triggered:

- 1) Route completed. The ego vehicle has finished all its target routes.
- 2) Route deviation. The ego vehicle deviates from its

target route far beyond 8m.

3) Collision. The ego vehicle collides with vehicles, walkers, or other static obstacles.

4) Timeout. The ego hasn't moved for over 50 seconds.

5) Traffic light/sign infraction. The ego vehicle runs a stop sign or a red light.

## 6.4. Reward Shaping.

Our reward is shaped to make the planner keep safe driving and finish the target route as much as possible, which consists of 4 parts:

1) Speed reward  $r_{speed}$  is used to train the ego vehicle to keep a safe speed, depending on the distance to other objects and their type.

2) Travel reward  $r_{travel}$  is the distance traveled along the target routes at each tick of CARLA. Travel reward encourages the ego vehicle to finish more target routes.

3) Deviation penalty  $p_{deviation}$  is the negative value of the distance between the ego vehicle and the lane center. It is normalized by the max deviation threshold  $D_{max}$ .

4) Steering cost  $c_{steer}$  is used to make the ego vehicle drive more smoother. We set it as a constant negative value and send it to the ego whenever the current steering is different from the last one.

The overall reward function is defined as follows:

$$r = \alpha_{sp} r_{speed} + \alpha_{tr} r_{travel} + \alpha_{de} p_{deviation} + \alpha_{st} c_{steer} \quad (7)$$

## 6.5. Model Size

Table 7. **Hyper-parameters of the neural network.** The CNN encoder maps the  $128 \times 128$  BEV to the  $4 \times 4$  feature map by  $4 \times 4$  convolutional kernel with stride 2. The flattened feature maps, concatenated with the state features output by the MLP encoder, are then input to the RSSM which consists of GRU cells and a few dense layers. The structure of the decoder inverts that of the encoder and outputs the reconstructed mask and state vector. Please refer to DreamerV3 [17] for details about network.

| GRU units | CNN multiplier | Dense hidden units | MLP layers | Params |
|-----------|----------------|--------------------|------------|--------|
| 512       | 96             | 512                | 5          | 104M   |

## 6.6. Hyperparameters of Training

Table 8. **Hyperparameter settings of training**

| Hyperparameters              | Notation         | Value                    |
|------------------------------|------------------|--------------------------|
| General                      |                  |                          |
| Replay capacity (FIFO)       | —                | 3e5                      |
| Batch size                   | $B$              | 16                       |
| Batch length                 | $T$              | 64                       |
| Activation                   | —                | LayerNorm + SiLU         |
| Reset step                   | —                | 0.8M                     |
| World Model Learning         |                  |                          |
| World model train ratio      | —                | 16                       |
| Reward prediction loss scale | —                | 10.0                     |
| Number of latents            | —                | 32                       |
| Classes per latent           | —                | 32                       |
| Reconstruction loss scale    | $\beta_{pred}$   | 1.0                      |
| Dynamics loss scale          | $\beta_{dyn}$    | 0.5                      |
| Representation loss scale    | $\beta_{rep}$    | 0.1                      |
| Learning rate                | —                | 1e-4                     |
| Adam epsilon                 | $\epsilon$       | 1e-8                     |
| Gradient clipping            | —                | 1000                     |
| Planner Learning             |                  |                          |
| Planner train ratio          | —                | 16, 32, 128, 256         |
| Imagination horizon          | —                | 15                       |
| Discount horizon             | $1/(1 - \gamma)$ | 333                      |
| Return lambda                | $\lambda$        | 0.95                     |
| Critic EMA decay             | —                | 0.98                     |
| Critic EMA regularizer       | —                | 1.0                      |
| Return normalization scale   | $S$              | $Per(R, 95) - Per(R, 5)$ |
| Return normalization limit   | —                | 1                        |
| Return normalization decay   | —                | 0.99                     |
| Actor entropy scale          | —                | 3e-4                     |
| Learning rate                | —                | 3e-5                     |
| Adam epsilon                 | $\epsilon$       | 1e-8                     |
| Gradient clipping            | —                | 100                      |
| Speed reward scale           | $\alpha_{sp}$    | 1.0                      |
| Travel reward scale          | $\alpha_{tr}$    | 1.0                      |
| Deviation reward scale       | $\alpha_{de}$    | 2.0                      |
| Steer cost scale             | $\alpha_{st}$    | 0.5                      |

## References

- [1] Yoshua Bengio, Jérôme Louradour, Ronan Collobert, and Jason Weston. Curriculum learning. In Proceedings of the 26th annual international conference on machine learning, pages 41–48, 2009. [5](#)
- [2] CARLA. Carla autonomous driving leaderboard, 2022. <https://leaderboard.carla.org/>. [1](#)
- [3] Raphael Chekroun, Marin Toromanoff, Sascha Hornauer, and Fabien Moutarde. Gri: General reinforced imitation and its application to vision-based autonomous driving. Robotics, 12(5):127, 2023. [2](#)
- [4] Dian Chen, Brady Zhou, Vladlen Koltun, and Philipp Krähenbühl. Learning by cheating. Conference on Robot Learning, Conference on Robot Learning, 2019. [3](#)
- [5] Jianyu Chen, Bodi Yuan, and Masayoshi Tomizuka. Model-free deep reinforcement learning for urban autonomous driving. In 2019 IEEE Intelligent Transportation Systems Conference (ITSC), 2019. [3](#)
- [6] Felipe Codevilla, Matthias Muller, Antonio Lopez, Vladlen Koltun, and Alexey Dosovitskiy. End-to-end driving via conditional imitation learning. In 2018 IEEE International Conference on Robotics and Automation (ICRA), 2018. [3](#)
- [7] Felipe Codevilla, Eder Santana, AntonioM. López, and Adrien Gaidon. Exploring the limitations of behavior cloning for autonomous driving. arXiv: Computer Vision and Pattern Recognition, arXiv: Computer Vision and Pattern Recognition, 2019. [3](#)
- [8] Alexey Dosovitskiy, German Ros, Felipe Codevilla, Antonio Lopez, and Vladlen Koltun. Carla: An open urban driving simulator. In Conference on robot learning, pages 1–16. PMLR, 2017. [1](#), [3](#)
- [9] Alexey Dosovitskiy, German Ros, Felipe Codevilla, AntonioM. López, and Vladlen Koltun. Carla: An open urban driving simulator. Conference on Robot Learning, Conference on Robot Learning, 2017. [3](#)
- [10] Scott Fujimoto, Herkevan Hoof, and David Meger. Addressing function approximation error in actor-critic methods. arXiv: Artificial Intelligence, arXiv: Artificial Intelligence, 2018. [3](#)
- [11] David Ha and Jürgen Schmidhuber. World models. arXiv preprint arXiv:1803.10122, 2018. [2](#)
- [12] Tuomas Haarnoja, Aurick Zhou, Pieter Abbeel, and Sergey Levine. Soft actor-critic: Off-policy maximum entropy deep reinforcement learning with a stochastic actor. arXiv: Learning, arXiv: Learning, 2018. [3](#)
- [13] Danijar Hafner, Timothy Lillicrap, Jimmy Ba, and Mohammad Norouzi. Dream to control: Learning behaviors by latent imagination. arXiv preprint arXiv:1912.01603, 2019. [2](#)
- [14] Danijar Hafner, Timothy Lillicrap, Ian Fischer, Ruben Villegas, David Ha, Honglak Lee, and James Davidson. Learning latent dynamics for planning from pixels. In International conference on machine learning, pages 2555–2565. PMLR, 2019. [2](#)
- [15] Danijar Hafner, Timothy Lillicrap, Ian Fischer, Ruben Villegas, David Ha, Honglak Lee, and James Davidson. Learning latent dynamics for planning from pixels. In Proceedings of the 36th International Conference on Machine Learning, pages 2555–2565. PMLR, 2019. [2](#)
- [16] Danijar Hafner, Timothy Lillicrap, Mohammad Norouzi, and Jimmy Ba. Mastering atari with discrete world models. arXiv preprint arXiv:2010.02193, 2020. [2](#)
- [17] Danijar Hafner, Jurgis Pasukonis, Jimmy Ba, and Timothy Lillicrap. Mastering diverse domains through world models, 2023. [2](#), [3](#), [4](#), [9](#)
- [18] Yihan Hu, Jiazhi Yang, Li Chen, Keyu Li, Chonghao Sima, Xizhou Zhu, Siqi Chai, Senyao Du, Tianwei Lin, Wenhai Wang, Lewei Lu, Xiaosong Jia, Qiang Liu, Jifeng Dai, Yu Qiao, and Hongyang Li. Planning-oriented autonomous driving. In Proceedings of the IEEE/CVF Conference on Computer Vision and Pattern Recognition, 2023. [1](#)
- [19] Ahmed Hussein, Mohamed Medhat Gaber, Eyad Elyan, and Chrisina Jayne. Imitation learning: A survey of learning methods. ACM Computing Surveys (CSUR), 50(2):1–35, 2017. [1](#)
- [20] Bernhard Jaeger, Kashyap Chitta, and Andreas Geiger. Hidden biases of end-to-end driving models. 2023. [1](#)
- [21] Xiaosong Jia, Liting Sun, Masayoshi Tomizuka, and Wei Zhan. Ide-net: Interactive driving event and pattern extraction from human data. IEEE Robotics and Automation Letters, 6(2):3065–3072, 2021. [1](#)
- [22] Xiaosong Jia, Peng Wu, Li Chen, Hongyang Li, Yu Sen Liu, and Junchi Yan. Hdgt: Heterogeneous driving graph transformer for multi-agent trajectory prediction via scene encoding. IEEE Transactions on Pattern Analysis and Machine Intelligence, 45:13860–13875, 2022.
- [23] Xiaosong Jia, Li Chen, Penghao Wu, Jia Zeng, Junchi Yan, Hongyang Li, and Yu Qiao. Towards capturing the temporal dynamics for trajectory prediction: a coarse-to-fine approach. In Proceedings of The 6th Conference on Robot Learning, pages 910–920. PMLR, 2023. [1](#)
- [24] Xiaosong Jia, Yulu Gao, Li Chen, Junchi Yan, Patrick Langechuan Liu, and Hongyang Li. Driveadapter: Breaking the coupling barrier of perception and planning in end-to-end autonomous driving. In Proceedings of the IEEE/CVF International Conference on Computer Vision, pages 7953–7963, 2023. [3](#)
- [25] Xiaosong Jia, Penghao Wu, Li Chen, Jiangwei Xie, Conghui He, Junchi Yan, and Hongyang Li. Think twice before driving: Towards scalable decoders for end-to-end autonomous driving. In Proceedings of the IEEE/CVF Conference on Computer Vision and Pattern Recognition, pages 21983–21994, 2023. [3](#)
- [26] Edouard Leurent. An environment for autonomous driving decision-making. <https://github.com/eleurent/highway-env>, 2018. [1](#)
- [27] Volodymyr Mnih, Koray Kavukcuoglu, David Silver, Alex Graves, Ioannis Antonoglou, Daan Wierstra, and Martin Riedmiller. Playing atari with deep reinforcement learning. arXiv preprint arXiv:1312.5602, 2013. [2](#)
- [28] Evgenii Nikishin, Max Schwarzer, Pierluca D’Oro, Pierre-Luc Bacon, and Aaron Courville. The primacy bias in deep reinforcement learning. In International conference on machine learning, pages 16828–16847. PMLR, 2022. [2](#), [4](#)

- [29] Nicholas Rhinehart, Rowan McAllister, and Sergey Levine. Deep imitative models for flexible inference, planning, and control. Computer Vision and Pattern Recognition, Computer Vision and Pattern Recognition, 2018. 3
- [30] Julian Schrittwieser, Ioannis Antonoglou, Thomas Hubert, Karen Simonyan, Laurent Sifre, Simon Schmitt, Arthur Guez, Edward Lockhart, Demis Hassabis, Thore Graepel, et al. Mastering atari, go, chess and shogi by planning with a learned model. Nature, 588(7839):604–609, 2020. 2
- [31] John Schulman, Filip Wolski, Prafulla Dhariwal, Alec Radford, and Oleg Klimov. Proximal policy optimization algorithms. arXiv preprint arXiv:1707.06347, 2017. 2, 6
- [32] Richard S Sutton, David McAllester, Satinder Singh, and Yishay Mansour. Policy gradient methods for reinforcement learning with function approximation. Advances in neural information processing systems, 12, 1999. 3
- [33] Martin Treiber, Ansgar Hennecke, and Dirk Helbing. Congested traffic states in empirical observations and microscopic simulations. Physical review E, 62(2):1805, 2000. 3
- [34] Hado Van Hasselt, Arthur Guez, and David Silver. Deep reinforcement learning with double q-learning. Proceedings of the AAAI Conference on Artificial Intelligence, 2022. 3
- [35] Penghao Wu, Xiaosong Jia, Li Chen, Junchi Yan, Hongyang Li, and Yu Qiao. Trajectory-guided control prediction for end-to-end autonomous driving: A simple yet strong baseline. Advances in Neural Information Processing Systems, 35:6119–6132, 2022. 3, 6
- [36] Penghao Wu, Li Chen, Hongyang Li, Xiaosong Jia, Junchi Yan, and Yu Qiao. Policy pre-training for autonomous driving via self-supervised geometric modeling. In International Conference on Learning Representations, 2023. 3
- [37] Philipp Wu, Alejandro Escontrela, Danijar Hafner, Pieter Abbeel, and Ken Goldberg. Daydreamer: World models for physical robot learning. In Conference on Robot Learning, pages 2226–2240. PMLR, 2023. 2
- [38] Zhejun Zhang, Alexander Liniger, Dengxin Dai, Fisher Yu, and Luc Van Gool. End-to-end urban driving by imitating a reinforcement learning coach. In Proceedings of the IEEE/CVF International Conference on Computer Vision (ICCV), 2021. 1, 2, 3, 4, 6